

## ARTICLE



# CC chemokine receptor 2 (CCR2) expression promotes diffuse large B-Cell lymphoma survival and invasion

Quan-Quan Hu<sup>1,4</sup>, Zhao-Feng Wen<sup>1,4</sup>, Qi-Tang Huang<sup>1</sup>, Qian Li<sup>2</sup>, Zhi-Min Zhai<sup>2</sup> and Yan-Li Li<sup>1,3</sup>✉

© The Author(s), under exclusive licence to United States and Canadian Academy of Pathology 2022

In recent years, CC chemokine receptor 2 (CCR2) has been found to be involved in tumor growth, angiogenesis, epithelial mesenchymal transition, metastasis, and immune escape. CCR2 overexpression was first identified as a poor prognostic predictor in diffuse large B-cell lymphoma (DLBCL) in our published article, but the mechanisms involved remain unknown. In this work, we collected data from another 138 patients with DLBCL data and verified the CCR2 expression level and its relationship to clinicopathological characteristics. Furthermore, we explored the possible mechanisms via in vitro and in vivo experiments. We showed that CCR2 overexpression was an independent prognostic marker and predicted shorter overall survival (OS) and progression-free survival (PFS) in patients with DLBCL. Blockade of CCR2 expression with a CCR2 antagonist inhibited tumor cell proliferation, migration, and anti-apoptosis ability in vitro by affecting the PI3K/Akt signaling pathway and the p38 MAPK signaling pathway. Furthermore, administration of a CCR2 antagonist decreased tumor growth and dissemination of DLBCL cells and increased survival time in the xenograft model. Our study demonstrates that CCR2 expression plays an important role in the development of DLBCL by stimulating cell proliferation, migration, and anti-apoptosis. Therefore, the inhibition of CCR2 may be a potential target for anticancer therapy in DLBCL.

*Laboratory Investigation* (2022) 102:1377–1388; <https://doi.org/10.1038/s41374-022-00824-5>

## INTRODUCTION

Diffuse large B-cell lymphoma (DLBCL) is the most common subgroup of non-Hodgkin lymphoma worldwide. It is a phenotypically and genetically heterogeneous disease, accounting for approximately 30–40% of all cases<sup>1,2</sup>. The addition of rituximab to standard CHOP (cyclophosphamide, doxorubicin, vincristine and prednisone) chemotherapy significantly increases event-free and overall survival (OS) times. Approximately 50–70% of DLBCL patients can be cured, but nearly one-third of patients develop relapsed or refractory disease that remains a major cause of mortality and morbidity due to the limited therapeutic options<sup>3–5</sup>. The prognosis of patients with newly diagnosed DLBCL depends on the prognostic clinical and biological characteristics as defined in the previously developed International Prognostic Index (IPI)<sup>6</sup>. The patient prognosis within the IPI group is highly variable; thus, novel biomarkers with potential implications for prognosis are of great importance<sup>7</sup>.

Chemokines that bind to receptors play an essential role in tumorigenesis and pathological immune pathways and have been investigated as markers of adverse prognosis in non-Hodgkin lymphomas<sup>8,9</sup>. CC chemokine receptor 2 (CCR2), a G protein-coupled receptor (GPCR) that mainly combines with CC ligand 2 (CCL2), can be detected in a diversity of cells, such as monocytes, memory T cells, natural killer (NK) cells, dendritic cells, and basophils<sup>10–13</sup>. The CCR2-CCL2 axis recruits inflammatory monocytes to the tumor microenvironment (TME) and promotes

polarization of selectively activated M2-phenotypes, thereby contributing to immunosuppression and enhancing tumor vascularization, cancer extravasation, and metastasis, including in prostate cancer, breast cancer, pancreatic cancer, and hepatocellular carcinoma<sup>13–18</sup>. This receptor and its ligands have been found to be involved in the tumor-promoting effects of malignant B cells in hematologic neoplasms such as follicular lymphoma<sup>19</sup>. In this study, we evaluated the prognostic significance of this receptor in patients with DLBCL and sought to investigate the role of alterations in CCR2 expression in DLBCL using in vitro and in vivo experiments.

## MATERIALS AND METHODS

### Patients and tissue samples

We recruited 138 patients with DLBCL who underwent pathological biopsies at the First Affiliated Hospital and the Second Affiliated Hospital of Anhui Medical University during the period from 2004–2016 based on the World Health Organization (WHO) criteria<sup>1</sup>, and all patients provided informed consent. The following criteria were met by all patients: pathologically substantiated DLBCL, no preceding history of malignancy, transplantation, or immunosuppression, and available laboratory data and follow-up information. All cases were evaluated for CCR2 expression by utilizing immunohistological analysis, and sections were independently reviewed by two highly experienced pathologists. Approximately 73% of patients were treated with the CHOP protocol, and 27% received the CHOP regimen plus rituximab as primary therapy and were followed-up at each

<sup>1</sup>Department of Pathology, School of Basic Medical Sciences, Anhui Medical University, Hefei 230032 Anhui, China. <sup>2</sup>Department of Hematology, The Second Affiliated Hospital of Anhui Medical University, Hefei 230601 Anhui, China. <sup>3</sup>Department of Pathology, The Second Affiliated Hospital of Anhui Medical University, Hefei 230601 Anhui, China. <sup>4</sup>These authors contributed equally: Quan-Quan Hu, Zhao-Feng Wen. ✉email: liyanli\_rainbow126@163.com

Received: 5 April 2022 Revised: 21 June 2022 Accepted: 21 June 2022  
Published online: 18 July 2022

of these two hospitals. This study was approved by the Institutional Review Board of Anhui Medical University and was conducted in accordance with The Code of Ethics of the World Medical Association (Declaration of Helsinki).

### Immunohistochemical staining

Specimens from 138 patients as well as subcutaneous tumors and infiltrated organs including bone marrow, lung, and central nervous system were fixed in 4% formalin and embedded in paraffin. We used 3  $\mu$ m paraffin sections and the monoclonal antibodies of CCR2 (1:300, Abcam, USA) for patient specimens and anti-human CD20 (ZSGB-Bio, Beijing, China), CCR2 (1:50, Bioss, Beijing, China) for subcutaneous tumors and infiltrated organs in the study. The sections were dewaxed in xylene and stripped of xylene in a gradient of ethanol to reduce water. Antigens were then repaired using sodium citrate solution (pH=6) using a high-pressure antigen repair method. After using 3% hydrogen peroxide to block endogenous peroxidase and goat serum to reduce non-specific background staining, anti-CD20 and CCR2 antibodies were incubated on the sections overnight at 4 °C. After recovery to room temperature, biotin-labelled secondary antibodies (anti-rabbit) were added dropwise for 30 min at 37 °C, followed by room temperature action using horseradish peroxidase-labelled ovalbumin for 15 min. Finally, DAB (ZSGB-Bio, Beijing, China) was used for color development, followed by staining using hematoxylin. The sections of subcutaneous tumors and disseminated organs were also stained with hematoxylin and eosin. Stained sections were interpreted by two professional pathologists, with different magnifications ( $\times 200$  and  $\times 400$ ) recorded in the same field of view for each section using an Olympus BX51TF microscope (Olympus, Tokyo, Japan). Semi-quantitative analysis of tumor cell staining was performed at grades 0, 1, 2, and 3. Grade 0 being < 1% tumor cell staining, grade 1 being 1–33%, grade 2 being 34–66%, and grade 3 being >67%. Grade 0 represented negative expression, and grades 1–3 represented positive expression<sup>20</sup>.

### Cell culture

SUDHL-4, SUDHL-6, and OCI-Ly8 (germinal center subtype, GCB) and SUDHL-2, OCI-Ly10 (activated subtype, ABC) are human-derived DLBCL cell lines. The SUDHL-2, SUDHL-4, and OCI-Ly10 cell lines were generously gifted by Dr. Ding (The First Affiliated Hospital Of USTC China), and the SUDHL-6 and OCI-Ly8 cell lines were presented by Prof. Zhai Zhimin (The Second Hospital Of Anhui Medical University, China). The cell culture media consisted of 1640 (Hyclone, Utah, USA) plus 10% fetal bovine serum (Gibco, NY, USA) and 1% penicillin/streptomycin (Beyotime, Shanghai, China). All cells were incubated at 37 °C in a 5% CO<sub>2</sub> incubator.

### Proliferation assays

Cell proliferation was measured using a Cell Counting Kit-8 (CCK8) (Beyotime, Shanghai, China). Briefly, SUDHL-2 and OCI-Ly8 cells were resuspended and then inoculated at  $3 \times 10^4$  cells/100  $\mu$ L in RPMI 1640 with 10% FBS media in 96-well plates. The CCR2 antagonist sc-202525 (50  $\mu$ M or 100  $\mu$ M, Santa Cruz Biotechnology, California, USA) was added, and the control group was treated with equal amounts of DMSO. The cells were incubated at 37 °C and 5% CO<sub>2</sub> for 24 h, 48 h, and 72 h; then, 10  $\mu$ L of CCK8 solution was added. After incubation at 37 °C for 2 h, the absorbance of each well at 450 nm was detected. Results represent the average absorbance of five wells  $\pm$  SD.

### Migration assay

Migration experiments were performed using 8- $\mu$ m pore size Transwell chambers (Corning Costar, NY, USA);  $2.5 \times 10^5$  cells in the upper chamber were resuspended in 100  $\mu$ L of serum-free medium with or without the CCR2 antagonist (100  $\mu$ M) and incubated for 2 h at 37 °C; 600  $\mu$ L of the serum-free medium was used in the lower chamber with or without rhMCP-1 (100 ng/ml, R&D System, California, USA), and the number of cells migrating to the lower chamber within 24 h was counted using a cell counting machine (JIMBIO-FIL, Jiangsu, China). Data represent the total number of cells that migrated to the lower chamber  $\pm$  the standard deviation (SD).

### Apoptosis analysis

To determine whether cells exposed to the CCR2 antagonist were undergoing apoptosis, we used an Annexin V-APC Apoptosis Assay Kit (BestBio, Beijing, China) according to the manufacturer's instructions and

detected the expression of cleaved caspase 3 protein by Western Blot (WB). In brief, SUDHL-2 cells and OCI-Ly8 cells were cultured in RPMI 1640 containing 10% FBS with the addition of the CCR2 antagonist (50  $\mu$ M or 100  $\mu$ M) for 48 h; then, the cells were collected for WB analysis or washed twice with PBS and incubated with 2  $\mu$ L of Annexin V-APC and 2  $\mu$ L of propidium iodide (PI) at 4 °C and protected from light for 0.5 h, then, they were probed by flow cytometry. The control group was processed with equal quantities of DMSO.

### Western blot analysis

The protein was extracted by centrifugation at 4 °C and 12,000 rpm/min for 20 min after collection and addition of RIPA (Beyotime, Shanghai, China) + 1% PMSF (Beyotime, Shanghai, China). The preparation of the BCA assay (Beyotime, Shanghai, China) for protein quantification was followed by adding a loading buffer (Beyotime, Shanghai, China) and boiling for 10 min. Approximately 20  $\mu$ g of proteins were separated by SDS polyacrylamide gel electrophoresis (SDS-PAGE), and the proteins were transferred to polyvinylidene difluoride (PVDF) membranes (Millipore, Massachusetts, USA). Following blocking of the membranes with 5% skim milk in Tris-saline buffer supplemented with 0.1% Tween-20 at room temperature for 1 h, they were subsequently treated with the primary antibodies at 4 °C overnight. The primary antibodies used were as follows: CCR2 antibody (1:1000, Bioworld Technology Inc., Minnesota, USA), cleaved caspase 3 antibody (1:500, Abcam, Cambridge, UK), p-PI3K antibody, p-Akt antibody, and p-p38 antibody (1:1000, all from Cell Signaling Technology, Boston, USA). After washing 3 times with TBST, the membranes were hatched with HRP-conjugated secondary antibody (1:5000, ZSGB-Bio, Beijing, China) for 1 h at room temperature. The bands were displayed using ECL reagent (Pierce, Massachusetts, USA) with a chemiluminescence imaging instrument (Tanon5200, Shanghai, China), and ImageJ software was used to analyze and calculate the grayscale values. The expression level of the objective protein was normalized to the level of  $\beta$ -actin (1:2000, ZSGB-Bio, Beijing, China).

### In vivo proliferation assay

Four-to-six-week-old BALB/c female nude mice (16–22 g) were obtained from GemPharmatech Co., Ltd. (Nanjing, China). Mice were housed in a specific pathogen-free (SPF) room under controlled temperature and humidity at the School of Basic Medical Sciences, Anhui Medical University. After a week of acclimatization,  $1.5 \times 10^7$  OCI-Ly8 cells were resuspended in 200  $\mu$ L of PBS and injected subcutaneously into the right axillary regions of the nude mice. When the tumor volume reached approximately 100 mm<sup>3</sup>, the mice were randomly divided into two groups: the CCR2 antagonist group ( $n = 5$ ) and the control group ( $n = 6$ ). The CCR2 antagonist group was injected intraperitoneally with the CCR2 antagonist at a dose of 10 mg/kg every other day, and the control group was given the same dose of DMSO every other day for 3 weeks (the day of administration was recorded as day 0). The weights of the mice and tumor size were recorded every other day, and the tumor volume was calculated as follows: (length  $\times$  width  $\times$  width)/2. When the tumor volume reached approximately 1500 mm<sup>3</sup>, mice were euthanized, and the tumors were removed. Tumor growth and changes in the weights of the mice were plotted as curves.

### In vivo migration assays and bioluminescent imaging

Four-to-six-week-old female NOD-SCID mice (16–20 g) were purchased from GemPharmatech Co., Ltd (Nanjing, China). Approximately  $1.5 \times 10^7$  Luciferin-labeled OCI-Ly8 cells were resuspended in 200  $\mu$ L of PBS and injected into the mice via the tail vein, followed by random division into the CCR2 antagonist group ( $n = 3$ ) and control group ( $n = 3$ ). The CCR2 antagonist group was administered the CCR2 antagonist (20 mg/kg) intraperitoneally every day, while the control group was given the same dose of DMSO intraperitoneally. We observed the statuses and weights of the mice daily. They were euthanized according to animal ethics when showing signs of metastasis such as straightened hair and significant weight loss. We monitored the dissemination of intravenously injected OCI-Ly8 cells via capturing bioluminescence images every 6 days using a bioluminescent imaging system (LagoHTX, USA). Mice were anesthetized with 3.5% isoflurane in oxygen, and bioluminescence images were captured 10 min after intraperitoneal injection of firefly D-luciferin (3 mg per mouse). The subcutaneous tumors and in vivo disseminated organs were removed for hematoxylin and eosin staining and immunohistochemical analysis. The animal experiments were approved by the Animal Ethics Committee of Anhui Medical University.

**Table 1.** Association between CCR2 expression and patients'clinico-pathological features.

clinico-pathological features	patients		CCR2 expression		
	N	%	Negative	Positive	P
Gender					
Male	73	53	17 (12)	56 (41)	0.427
Female	65	47	19 (14)	46 (33)	
Age					
Median (range)	58 (13–84)				
<60	80	58	24 (17)	56 (41)	0.219
≥60	58	42	12 (9)	46 (33)	
Ann Arbor stage					
I/II	67	49	27 (20)	40 (29)	<0.001**
III/IV	71	51	9 (6)	62 (45)	
Extranodal sites of disease					
≤1	101	73	30 (22)	71 (51)	0.110
> 1	37	27	6 (4)	31 (23)	
ECOG					
≤1	79	57	25 (18)	54 (39)	0.085
> 1	59	43	11 (8)	48 (35)	
LDH					
<normal	91	66	33 (24)	58 (42)	<0.001**
≥normal	47	34	3 (2)	44 (32)	
IPI					
0-2	84	61	30 (22)	53 (39)	0.001*
3-5	54	39	6 (4)	48 (35)	
Chemotherapy					
CHOP	101	73	24 (17)	77 (56)	0.304
R-CHOP	37	27	12 (9)	25 (18)	
Subtype1					
ABC	79	57	19 (14)	60 (44)	0.528
GCB	59	43	17 (12)	42 (30)	

ECOG Eastern Cooperative Group, LDH Lactate dehydrogenase, IPI International Prognostic Index. 1 Hans algorithm was used to determine the GCB/Non-GCB cases. *P*-values were calculated using Fisher's exact test. \**P* < 0.05, \*\**P* < 0.01.

### Statistical analysis

All data values are reported as the mean ± SEM from three independent experiments. We used either the chi-square test or Fisher's exact test to compare categorical values between the two groups. Univariate and multivariate analyses for progression-free survival (PFS) and OS were performed using the Cox proportional hazard model. Survival curves were constructed using the Kaplan-Meier method, and log-rank tests were used to compare differences between the groups. For the cell culture trials and in vivo experiments, we determined statistical significance by two-tailed Student's *t*-tests using GraphPad Prism (version 8.0.2). The statistical calculations were conducted using SPSS software (version 25). *P* < 0.05 indicates a statistically significant result.

## RESULTS

### Immunohistochemical CCR2 intensity and its correspondence with clinicopathological features

We performed an assessment of CCR2 expression in 138 biopsies from patients with DLBCL. All the clinical data of the enrolled DLBCL patients are available in Table 1. A high expression of CCR2 was observed in 102 cases (74%) and is expressed in tumor cells in both the cytoplasm and cell membrane (Fig. 1A, B). The frequency of CCR2 expression progressively increased with higher IPI scores (Table 1, *P* = 0.001). Positive CCR2 expression in patients with

DLBCL was remarkably correlated with Ann Arbor stage and LDH (Table 1, *P* < 0.001, respectively).

### High CCR2 expression is a negative prognostic factor affecting OS and PFS in patients with DLBCL

To examine whether CCR2 expression is an independent prognostic predictor of PFS and OS, we performed univariate and multivariate Cox regression analysis. By employing univariate Cox analysis, as shown in Table 2 and Table 3, CCR2 expression was found to be a statistically significant predictor of PFS (HR:14.527, *P* < 0.001) and OS (HR:5.419, *P* < 0.001). The same was true for LDH (HR:1.969, *P* = 0.047 for PFS and HR:2.353, *P* = 0.018 for OS). In addition, ECOG was an independent prognostic factor for PFS (HR:0.561, *P* = 0.047). Furthermore, multivariate Cox analysis revealed that CCR2 expression and LDH remained significant prognostic factors for PFS (Table 2, HR:11.002, *P* < 0.001 and HR:2.337, *P* = 0.006, respectively). Similarly, CCR2 expression and LDH were demonstrated to be significant prognostic factors for OS (Table 3, HR:4.670, *P* < 0.001 and HR:2.231, *P* = 0.011, respectively). Following first-line chemotherapy, the overall effectiveness rate including complete response (CR) and partial response (PR) was 63% in our research. The significant effect of CCR2 expression on the overall response rate is shown in Table 4 (*P* < 0.001). In

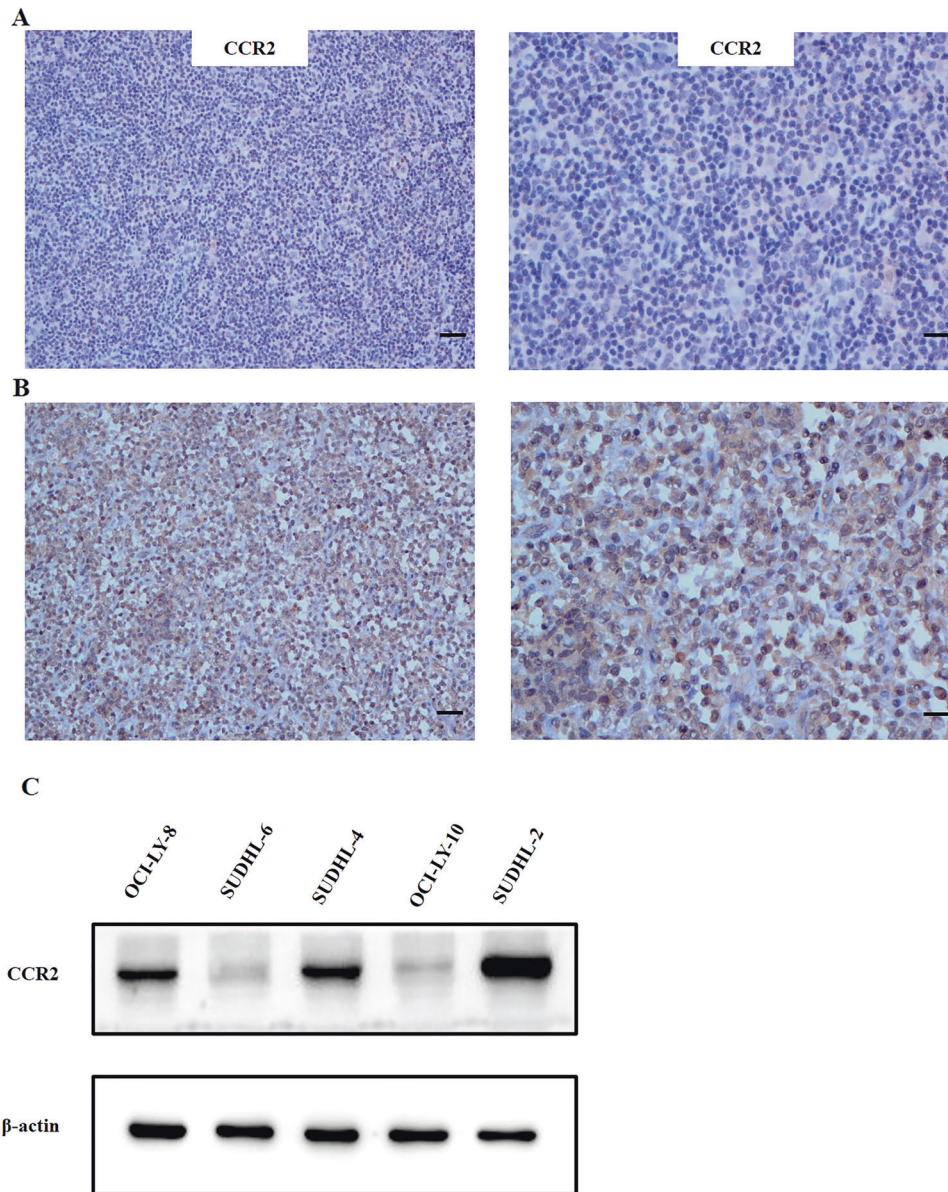


**Fig. 1** Expression of CCR2 in DLBCL tissues and cell lines. **A** Low cytoplasmic or membrane staining of CCR2. Original magnification x200 and x400. Scale bar, 50  $\mu$ m and 20  $\mu$ m. **B** High cytoplasmic or membrane staining of CCR2. Original magnification x200 and x400. Scale bar, 50  $\mu$ m, and 20  $\mu$ m. **C** CCR2 were expressed in human DLBCL cell lines of SUDHL-2, SUDHL-4, SUDHL-6, OCI-Ly8, and OCI-Ly10.

addition, in different treatment cohorts, we found that there was no significant correlation between the expression of CCR2 and cell origin (COO) (Table 5). Kaplan-Meier analysis indicated that patients with CCR2-positive expression ( $n = 102$ ) had significantly poorer PFS (Fig. 2A, log-rank  $P < 0.001$ ) and OS (Fig. 2E, log-rank  $P < 0.001$ ) than those with CCR2-negative expression. We further investigated whether CCR2 expression could stratify low-risk (IPI score = 0–1), intermediate-risk (IPI score = 2–3), and high-risk (IPI score = 4–5) patients. CCR2 expression significantly stratified patients when the analysis was limited to low- and intermediate-risk patients (Fig. 2B, C, PFS:  $P < 0.001$  and  $P = 0.001$ , respectively; Fig. 2F, G, OS:  $P < 0.001$  and  $P < 0.001$ , respectively). Nevertheless, in our study, CCR2 expression was not predictive of high-risk DLBCL (Fig. 2D, PFS:  $P = 0.051$ ; Fig. 2H, OS:  $P = 0.448$ ). Furthermore, received R-CHOP patients with high CCR2 ( $n = 25$ ) expression had significantly poorer PFS (Fig. 2I, log-rank  $P < 0.001$ ) and OS

(Fig. 2J, log-rank  $P < 0.001$ ) than those with low CCR2 ( $n = 12$ ) expression, respectively.

#### Association of CCR2 expression with proliferation and migration in DLBCL cells

We evaluated CCR2 expression in DLBCL cell lines by Western blot analysis and found that CCR2 was expressed in all cell lines to different degrees (Fig. 1C, D). To verify the effect of the CCR2 expression level on the proliferation of DLBCL cells, SUDHL-2 and OCI-Ly8 cells were supplemented with a CCR2 antagonist (sc-202525, 50  $\mu$ M or 100  $\mu$ M) or DMSO (equal in volume to the CCR2 antagonist treatment). We found that sc-202525 significantly inhibited the proliferation rate of SUDHL-2 (Fig. 3A,  $P < 0.01$ ) and OCI-Ly8 cells (Fig. 3B,  $P < 0.01$ ) compared with DMSO treatment. To identify of the migratory impact of CCR2 expression, we evaluated the migration induced by MCP-1 in DLBCL cell lines. Recombinant human (rh)MCP-1 (100 ng/ml) was added to the

**Table 2.** Univariate and multivariate COX regression analysis for progression-free survival in DLBCL patients.

Variables	Progression-free survival			
	Univariate COX Regression		Multivariate COX Regression	
	HR (IC 95%)	P	HR (IC 95%)	P
CCR2 (+/-)	14.527 (6.692–31.536)	<0.001**	11.002 (5.285–22.903)	<0.001**
LDH (Normal/High)	1.969 (1.008–3.848)	0.047*	2.337 (1.274–4.289)	0.006**
ECOG ( $\leq 1/\text{> } 1$ )	0.561 (0.317–0.993)	0.047*	0.642 (0.395–1.044)	0.074
IPI (0-2/3-5)	1.063 (0.356–3.175)	0.913		
Ann Arbor stage (I-II/III-IV)	0.687 (0.351–1.345)	0.273		
Extranodal sites of disease ( $\leq 1/\text{> } 1$ )	1.993 (0.788–5.045)	0.145		
GCB (yes/no)	0.625 (0.387–1.012)	0.056		
Age (<60/ $\geq 60$ )	1.270 (0.770–2.096)	0.349		
CHOP/R-CHOP	1.405 (0.878–2.248)	0.156		

Only significant factors for the univariate analysis were included in the multivariate analysis. HR Hazard ratio, 95% IC 95% confidence interval of hazard ratio, LDH Lactate dehydrogenase, ECOG Eastern Cooperative Group, IPI International Prognostic Index. \* $P < 0.05$ , \*\* $P < 0.01$ .

**Table 3.** Univariate and multivariate COX regression analysis for overall survival in DLBCL patients.

Variables	Overall survival			
	Univariate COX Regression		Multivariate COX Regression	
	HR (IC 95%)	P	HR (IC 95%)	P
CCR2 (+/-)	5.419 (3.038–9.668)	<0.001**	4.670 (2.698–8.083)	<0.001**
LDH (Normal/High)	2.353 (1.160–4.776)	0.018*	2.231 (1.206–4.129)	0.011*
ECOG ( $\leq 1/\text{> } 1$ )	0.931 (0.538–1.611)	0.931		
IPI (0-2/3-5)	0.713 (0.212–2.397)	0.585		
Ann Arbor stage (I-II/III-IV)	0.653 (0.338–1.263)	0.206		
Extranodal sites of disease ( $\leq 1/\text{> } 1$ )	1.675 (0.699–4.017)	0.248		
GCB (yes/no)	0.839 (0.520–1.353)	0.471		
Age (<60/ $\geq 60$ )	0.841 (0.496–1.426)	0.521		
CHOP/R-CHOP	1.364 (0.852–2.183)	0.196		

Only significant factors for the univariate analysis were included in the multivariate analysis. HR Hazard ratio, 95% IC 95% confidence interval of hazard ratio, LDH Lactate dehydrogenase, ECOG Eastern Cooperative Group, IPI International Prognostic Index. \* $P < 0.05$ , \*\* $P < 0.01$ .

**Table 4.** Response rate according to CCR2 expression.

Characteristic	Response		Response rate	
	CR/PR	PD	%	P
CCR2				
Negative	32	4	89	<0.001**
Positive	55	47	54	<0.001**

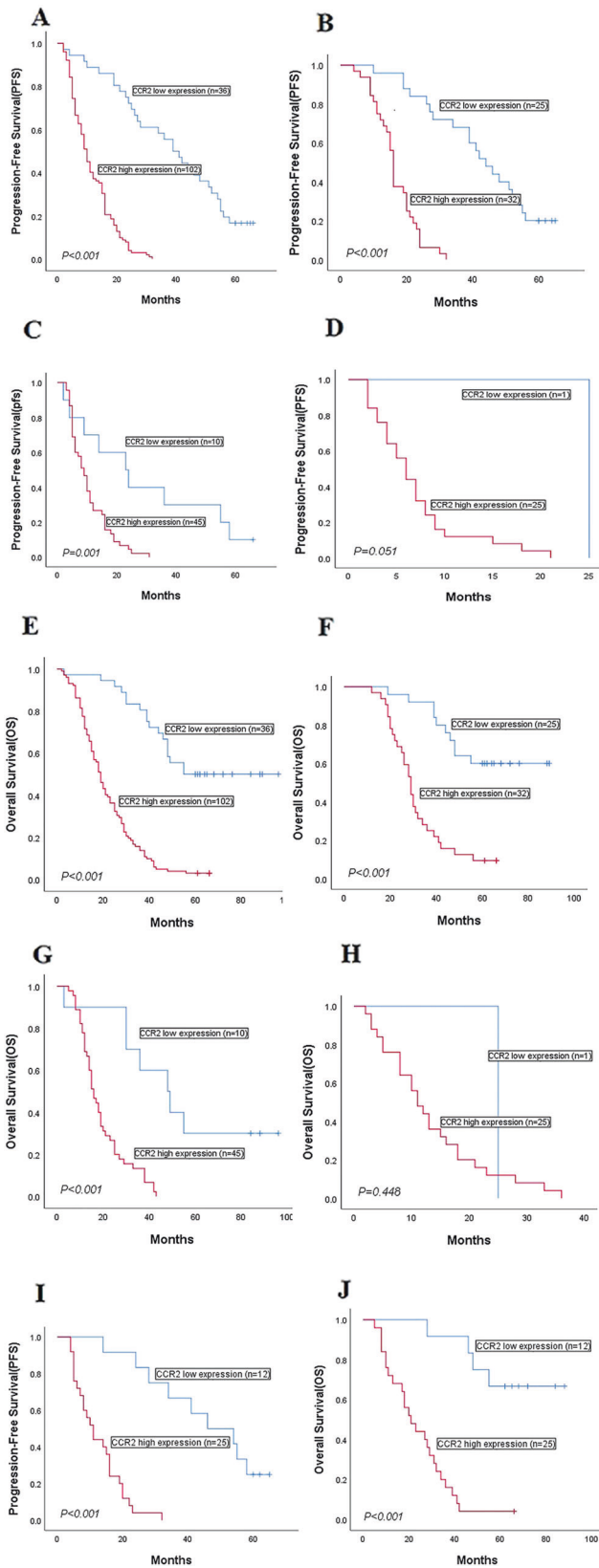
CR Complete response, PR Partial response, PD Progressive disease. \*\* $P < 0.01$ .

lower chamber to stimulate cell migration, and OCI-Ly8 cells showed increased migration capacity in the presence of MCP-1. However, there was no difference in SUDHL-2 cells. To evaluate whether MCP-1-driven migration was dependent on CCR2 expression, we evaluated whether exposure to sc-202525, a

**Table 5.** The correlation between CCR2 expression and COO in different treatment cohorts.

Characteristic	CCR2		P
	Negative	Positive	
CHOP			
ABC	12	90	0.288
GCB	12	64	
R-CHOP			
ABC	7	30	0.582
GCB	5	20	

CCR2 antagonist, repressed this migration. We found that sc-202525 significantly inhibited migration of SUDHL-2 and OCI-Ly8 cell lines (Fig. 3C).



### CCR2 expression promotes the anti-apoptotic ability of DLBCL cells

To ascertain whether CCR2 activates intracellular signals, a CCR2 antagonist (sc-202525) was applied to SUDHL-2 and OCI-Ly8 cells for

**Fig. 2** Kaplan-Meier analysis of PFS and OS according to the expression of CCR2 in patients with DLBCL. **A** Kaplan-Meier analysis of PFS of all patients ( $P < 0.001$ ). **B** Kaplan-Meier analysis of PFS of patients with IPI score = 0–1 ( $P < 0.001$ ). **C** Kaplan-Meier analysis of PFS of patients with IPI score = 2–3 ( $P = 0.001$ ). **D** Kaplan-Meier analysis of PFS of patients with IPI score = 4–5 ( $P = 0.051$ ). **E** Kaplan-Meier analysis of OS of all patients ( $P < 0.001$ ). **F** Kaplan-Meier analysis of OS of patients with IPI score = 0–1 ( $P < 0.001$ ). **G** Kaplan-Meier analysis of PFS of patients with IPI score = 2–3 ( $P < 0.001$ ). **H** Kaplan-Meier analysis of PFS of patients with IPI score = 4–5 ( $P = 0.448$ ). **I** Kaplan-Meier analysis of PFS of patients with R-CHOP therapy ( $P < 0.001$ ). **J** Kaplan-Meier analysis of OS of patients with R-CHOP therapy ( $P < 0.001$ ).  $P$ -values were calculated using the Log-rank test.

48 h. Then, cell apoptosis was detected by flow analysis using an apoptosis reagent kit and observed the expression of cleaved caspase 3 protein by WB analysis. The same amount of DMSO was substituted for the negative group. As the illustration demonstrates, apoptosis increased after treatment with sc-202525, and the apoptosis rates of SUDHL-2 (Fig. 4A,  $P < 0.01$ ) and OCI-Ly8 cells (Fig. 4B,  $P < 0.01$ ) were approximately 3.5 times and 7 times higher, respectively, than those of the control group. Similarly, Fig. 4C shows that the expression of cleaved caspase 3 was higher in DLBCL cells affected by CCR2 antagonists compared to the control group ( $P < 0.01$ ).

### CCR2 activates the PI3K-Akt MARK signaling pathway and inhibits the p38 MAPK signaling pathway in DLBCL

The published literature has reported that the expression of the PI3K/Akt and p38 MAPK signaling pathways in prostate cancer and breast cancer are correlated with the level of CCR2<sup>21</sup>. However, the role of these signaling pathways in DLBCL has not been previously reported. To gain further insights into the molecular mechanism by which CCR2 facilitates DLBCL cell survival, we treated SUDHL-2 and OCI-Ly8 cells with sc-202525 for 48 h and then screened for p-PI3K protein, p-Akt protein, p-p38 protein, p-STAT3 protein, p-STAT5 protein, p-Src protein, p-P44/42 protein, and p-NF- $\kappa$ B protein expression by Western blot analysis. We observed that the expression levels of p-PI3K and p-Akt expression were dramatically decreased, whereas those of p-p38 protein were significantly increased in both strains of cells (Fig. 4D, E). The PI3K/Akt and p38 MAPK signaling pathways are engaged in regulating cell proliferation, metabolism, and motility<sup>22–24</sup>. We suggest that CCR2 expression is involved in the proliferation and migration of DLBCL cells by activating the PI3K/Akt signaling pathway and CCR2 antagonist induces apoptosis through activation of the p38 MAPK signaling pathway.

### CCR2 antagonists inhibit subcutaneous tumor growth by blocking CCR2

Based on the results of the in vitro experiments, we performed in vivo experiments to explore whether a CCR2 antagonist could inhibit tumor growth by blocking CCR2 in vivo. We transplanted  $1.5 \times 10^7$  OCI-Ly8 cells into the right axillary subcutis of nude mice. When a tumor was apparent, the mice were randomly divided into two groups. The CCR2 antagonist group was administered a CCR2 antagonist (10 mg/kg), and the control group was given the same dose of DMSO every other day. We recorded the weights of the mice and subcutaneous tumor size every other day. The results showed that the tumor size and tumor weight in mice treated with the CCR2 antagonist were significantly reduced compared with those in mice in the control group (Fig. 5A–C, E); however, the body weights of the mice showed no significant difference between the two groups (Fig. 5D). When the subcutaneous tumor volume reached approximately 1500 mm<sup>3</sup>, the mice were euthanized, and the tumors were removed and weighed. Immunohistochemistry and hematoxylin and eosin staining were performed on the subcutaneous tumors of mice from both groups; CCR2 and

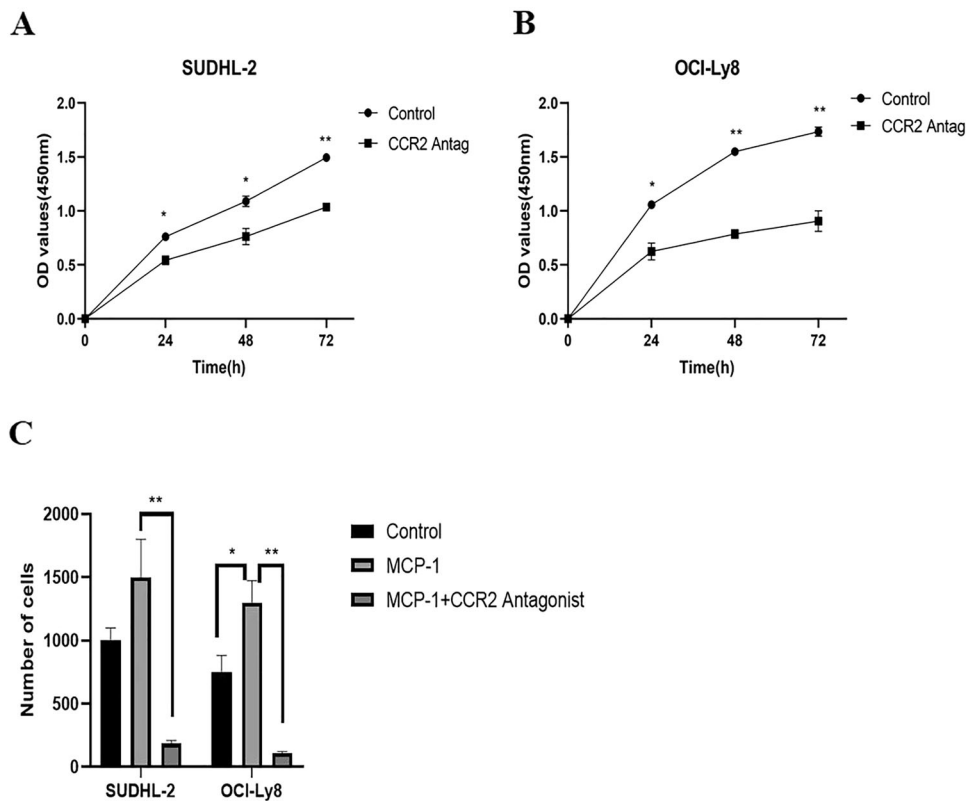


**Fig. 3 CCR2 expression driven the proliferation and migration in DLBCL cell lines.** **A** SUDHL-2 cells. **B** OCI-Ly8 cells. To determine growth, SUDHL-2 or OCI-Ly8 cells ( $2 \times 10^4$ /well) were seeded into a 96-well plate and cultured for 24–72 h with RPMI 1640 and 10% fetal bovine serum and relative cell numbers in each well measured by CCK8. Cells were grown in the presence of CCR2 antagonist sc-202525. The control cells were treated with equivalent amounts of DMSO. **C** Association of CCR2 expression with MCP-1 driven migration in DLBCL cell lines. To determine migration, cells were incubated in serum-free media in the presence or absence of CCR2 antagonist sc-202525 (100  $\mu$ M) prior to and during the transwell migration assay. Recombinant human (rh) MCP-1 (100 ng/ml) was added to the lower chamber to stimulate cell migration. Cells unexposed to rhMCP-1 were used as control. OCI-Ly8 cell increased their migration capacity in the presence of MCP-1, however there was no difference in SUDHL-2 cells. We found that sc-202525 significantly inhibited migration spurred by MCP-1 in SUDHL-2 and OCI-Ly8 cell lines. Data are presented as the mean  $\pm$  SEM ( $n = 3$ ). \* $P < 0.05$ , \*\* $P < 0.01$ .

CD20 expression was significantly decreased in the CCR2 antagonist-treated group compared with the DMSO-treated group, and we observed necrotic tumor cells and residual tumor cells from the IHC image of CCR2 in the CCR2 antagonist-administered group (Fig. 5F). These results confirmed that CCR2 antagonist treatment can inhibit the growth of the subcutaneous tumors by blocking CCR2.

### CCR2 antagonists significantly inhibit tumor dissemination

We have shown that a CCR2 antagonist inhibited tumor growth by blocking CCR2. Thus, we next explored whether treatment with a CCR2 antagonist could inhibit tumor dissemination in vivo. Approximately  $1.5 \times 10^7$  OCI-Ly8 cells were resuspended in 200  $\mu$ l of PBS and injected intravenously into NOD-SCID mice. The mice were then randomly divided into two groups; one group was administered a CCR2 antagonist (20 mg/kg) intraperitoneally daily, and the control group was administered intraperitoneal DMSO. Bioluminescence imaging was performed every 6 days to monitor the dissemination of tumors in the mice. On day 12, a significant difference in tumor dissemination began to appear between the two groups, with parenchymal organ dissemination in the control group. The difference in dissemination between the two groups became gradually more pronounced (Fig. 6A). Bioluminescence images were analyzed using software to obtain the fluorescence intensity of the tumor-disseminated organs, and it showed that the intensity of the control group increased significantly, with a significant difference between the two groups (Fig. 6B). The mice were euthanized when they showed straightened hair and

significant weight loss. Then, all the organs of mice in the control group were removed for hematoxylin and eosin and immunohistochemical staining. Finally, the bone marrow and central nervous systems of the control mice were found to be seeded by the tumors, which was consistent with the bioluminescence imaging findings (Fig. 6C). These results confirmed that treatment with a CCR2 antagonist could inhibit tumor dissemination in vivo.

### DISCUSSION

In the current study, we investigated the prognostic significance of CCR2 expression in patients with DLBCL. We found that CCR2 was highly expressed in 74% of patients with DLBCL and that the frequency of CCR2 expression gradually increased with increasing IPI scores. In addition, through multivariate analysis, we found that CCR2 was an independent prognostic marker affecting patients with DLBCL patients. These findings are consistent with the statistical results of our pre-published clinical materials<sup>20</sup>. Furthermore, our findings are paralleled by those of previous studies in which CCR2 expression was described as a prognostic factor associated with poor prognosis in liver, lung, prostate, colorectal, and renal cancer<sup>13,25–29</sup>. Furthermore, Kaplan-Meier analysis showed that patients with positive CCR2 expression had markedly inferior PFS and OS, which is consistent with the observations of B. Ou et al.<sup>28</sup>.

Since CCR2 expression was upregulated in the majority of patients with DLBCL, we investigated the expression of CCR2 in DLBCL cell lines to explore the role of this receptor on DLBCL cells. The results of the in vitro studies showed that CCR2 expression

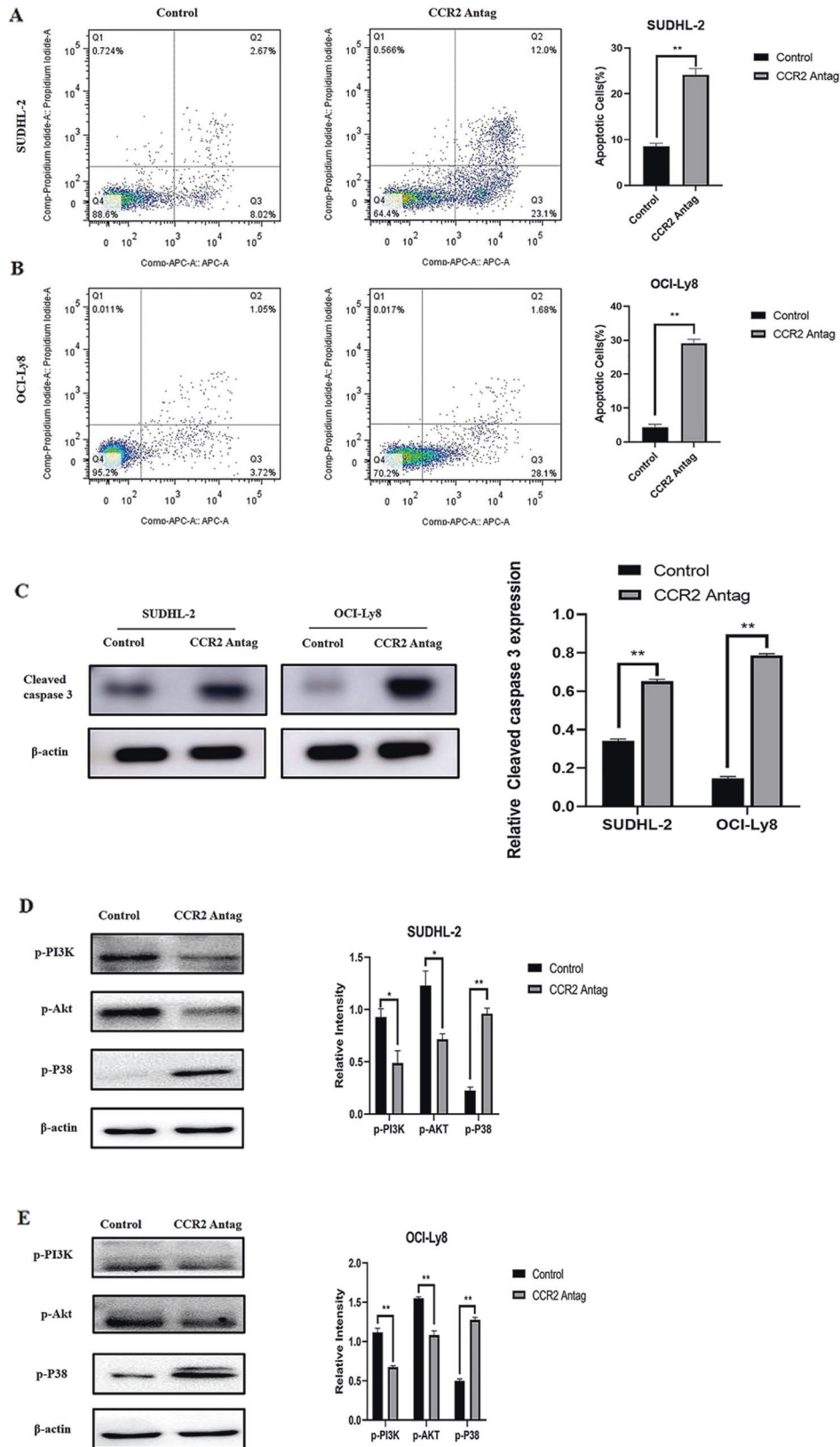


**Fig. 4 CCR2 expression promotes anti-apoptotic ability and signalling pathways associated with biological behavior in DLBCL.** **A** To determine apoptotic, SUDHL-2 cells (**A**) and OCI-Ly8 cells (**B**) either treated with DMSO (Control) or after treatment with 50  $\mu$ M sc-202525 for 48 h and cell viability was measured by FACS used Annexin V APC-PI Apoptosis kit and detected the expression of cleaved caspase 3 protein by WB (**C**). To obtain a deeper understanding of the molecular mechanisms of CCR2 on DLBCL cells, we treated SUDHL-2 cells (**D**) and OCI-Ly8 cells (**E**) with sc-202525 for 48 h, detection p-Pi3K protein, p-Akt protein, p-protein, p-STAT3 protein, p-STAT5 protein, p-Src protein, p-P44/42 protein and p-NF- $\kappa$ B protein expression by Western Blotting. Cells dealt with CCR2 antagonist p-Pi3K and p-Akt expression decreased, however p-p38 protein express raised vs. the control cells (treated with DMSO). Data are presented as the mean  $\pm$  SEM. \* $P$  < 0.05, \*\*\* $P$  < 0.01.



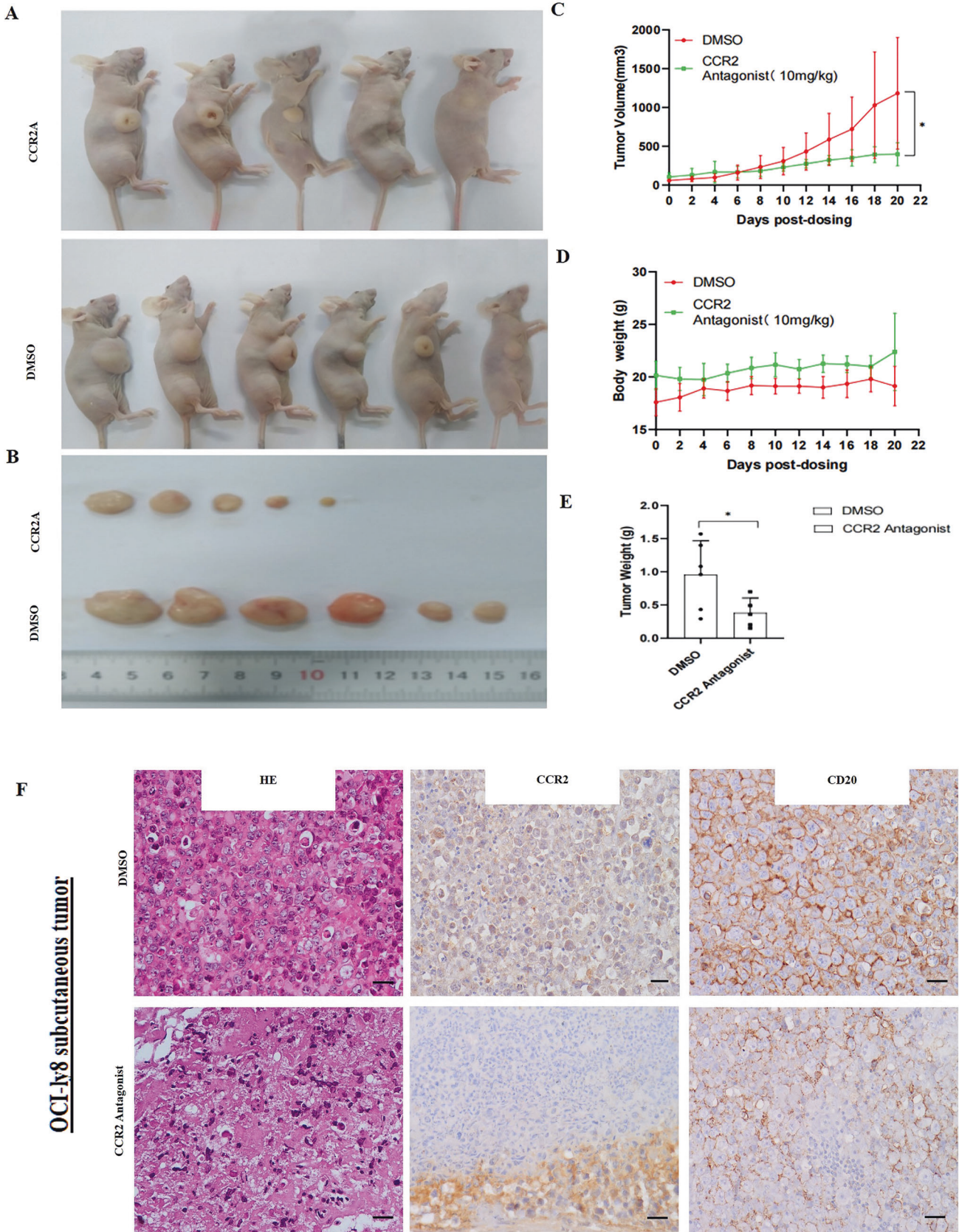


**Fig. 5 CCR2 antagonist inhibits the growth of subcutaneous tumor.**  $1.5 \times 10^7$  OCI-ly8 cells were transplanted into the right sides of nude mice. When tumor volume reached about  $100 \text{ mm}^3$ , we divided the mice into two groups, which administrated CCR2 antagonist (10 mg/kg) or DMSO intraperitoneally every other day. **A** Representative images of subcutaneous tumors treated with CCR2 antagonist or DMSO. **B** Subcutaneous tumors were removed from euthanized mice. **C** The tumor volumes of two groups (means  $\pm$  SEM; CCR2 antagonist,  $n = 5$ ; DMSO,  $n = 6$ ;  $*P < 0.05$ ). **D** The mice weight of two groups (means  $\pm$  SEM). **E** The subcutaneous tumor weights of two groups (means  $\pm$  SEM,  $*P < 0.05$ ). **F** H&E staining and immunohistochemistry (CCR2 and CD20) were performed on OCI-ly8 subcutaneous tumors after CCR2 antagonist treatment. Scale bar, 20  $\mu\text{m}$ ; original magnification  $\times 400$ . H&E, hematoxylin and eosin staining.

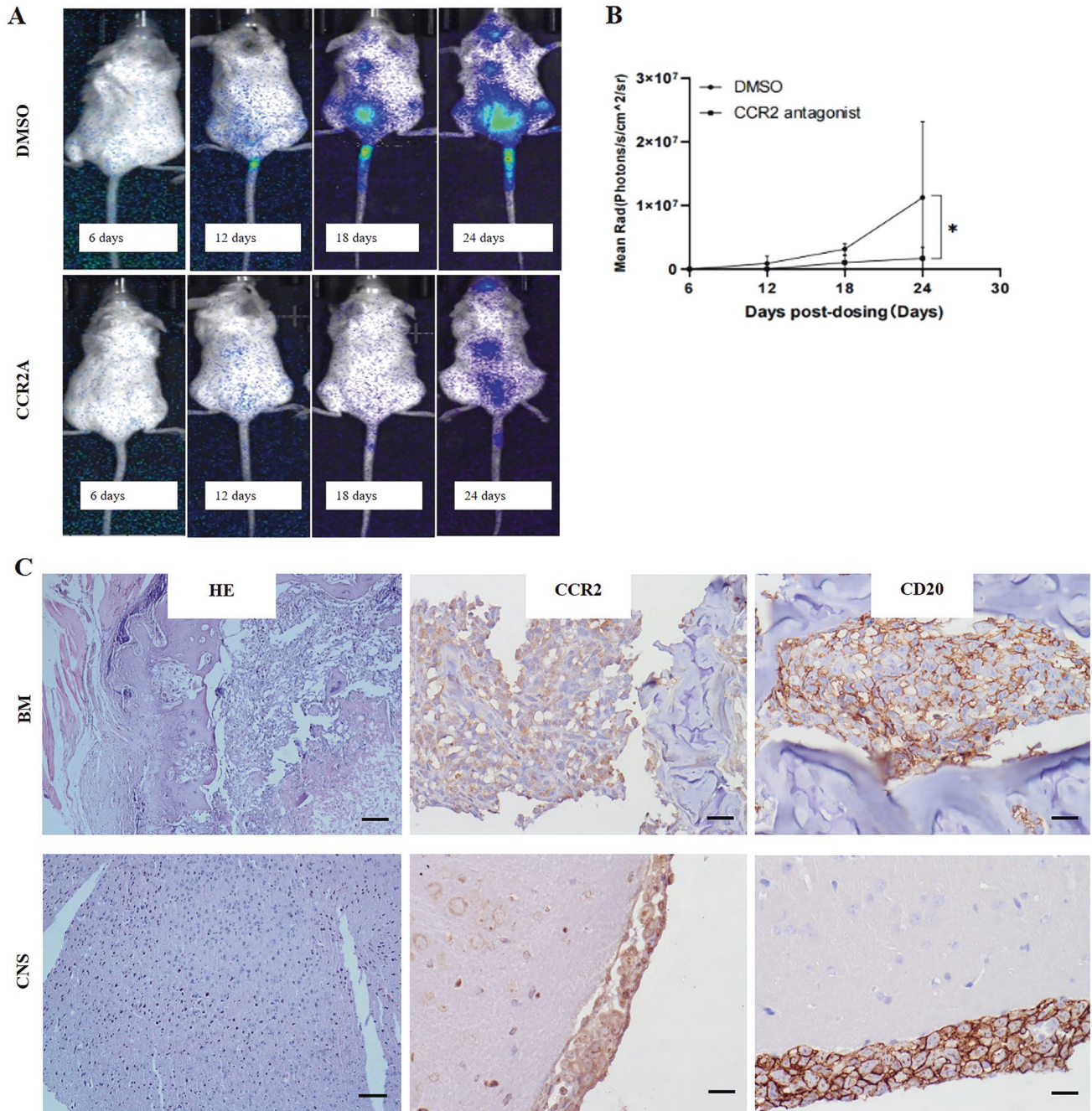


**Fig. 6 CCR2 antagonist inhibits the dissemination of tumor.**  $1.5 \times 10^7$  OCI-ly8 cells were injected intravenously into NOD-SCID mice, which were intraperitoneally dosed daily with CCR2 antagonist (20 mg/kg) or DMSO. The tumor dissemination was monitored through bioluminescent imaging (BLI) every six days. After 24 days, the mice were euthanized and removed all organs for H&E and immunohistochemistry. Finally, we found the BM and CNS were disseminated organs with being consistent with the BLI. **A** The BLI of CCR2 antagonist ( $n = 3$ ) or DMSO ( $n = 3$ ) treated mice. **B** The BLI curve of CCR2 antagonist or DMSO treated mice (means  $\pm$  SEM, which statistical test  $*P < 0.05$ ). **C** The expression of CD20 and CCR2 of BM and CNS of the disseminated mice. Scale bar, 20  $\mu\text{m}$ ; original magnification  $\times 400$ . H&E Hematoxylin and eosin staining, BM Bone marrow, CNS Central nervous system.

was detected in a protein-level analysis in DLBCL cell lines including SUDHL-2, SUDHL-4, OCI-Ly10, SUDHL-6, and OCI-LY8 cells. Several published studies have identified the expression of CCR2 in cancer cells, including prostate cancer<sup>27</sup>, multiple myeloma<sup>30</sup>, renal cancer<sup>29</sup>, and lung cancer cell lines<sup>26</sup>. To examine the immediate effects of CCR2 expression on DLBCL cell lines in an in vitro experiment, we treated SUDHL-2 and OCI-Ly8 cells with pharmacological concentrations of the CCR2 antagonist sc-202525. The results indicate that a high level of CCR2 stimulates the proliferation, migration, and anti-apoptotic abilities of DLBCL cells. The present results are consistent with those of previous studies in which CCR2 expression was found to facilitate the neoplastic progression of colorectal and ovarian cancer<sup>28,31</sup>.

In the in vivo experiments, the results showed that the tumor volume was significantly reduced after treatment with a CCR2 antagonist, and bioluminescence imaging indicated that CCR2 antagonists significantly inhibit DLBCL cell dissemination. These results are consistent with our in vitro observations. Due to the important role of CCR2 in tumor growth, invasion, migration, and survival, the optimal use of CCR2 inhibition may be part of a potential targeted therapy. The results of the current study indicate that CCR2 antagonists reduce cell viability, block metastasis, improve chemotherapeutic efficacy, and overcome macrophage-induced depression<sup>17,32,33</sup>. A potent, selective and orally administered CCR2 antagonist, designated INCB3344, has been evaluated previously in both humans and mice<sup>34</sup>. In fact, a phase II clinical trial was performed using the anti-CCR2 monoclonal antibody MLN1202 in patients with bone metastasis from cancer<sup>35</sup>. In addition, Chemocentryx has recently commenced a Phase Ib trial of a CCR2 antagonist (CCX872) for the treatment of patients with unresectable pancreatic cancer<sup>36</sup>. These clinical studies will provide important information on the safety and potential therapeutic effects of a CCR2 signaling blockade in patients with cancer.

The PI3K/Akt and p38 MAPK signaling pathways are critical for many physiological and pathological conditions, such as regulating cell survival, growth, proliferation, angiogenesis, transcription, translation, and metabolism<sup>21,37–39</sup>. To further investigate the molecular mechanisms by which CCR2 expression promotes the survival of DLBCL cells, WB analysis for the PI3K/Akt and p38 MAPK signaling pathways showed that CCR2 antagonists significantly inhibited the activation of the PI3K/Akt signaling pathway but activated the p38 MAPK signaling pathway in vitro. Similarly, Roca et al. found that the CCL2-CCR2 axis regulates autophagy and increases survivin expression via the PI3K/Akt pathway, providing a strong survival advantage in PC-3 prostate cancer cells<sup>40</sup>. In ovarian cancer, Chao et al. found that binding of large omental adipocytes to their cognate receptor CCR2 promotes tumor cell migration and omental metastasis through activation of the PI3K/Akt pathway<sup>31</sup>. In addition, Erwin F et al. found that apoptotic stimuli sometimes trigger the activation of p38 via secondary pathways, such as the production of reactive oxygen species (ROS)<sup>21</sup>. These results highly emphasize the carcinogenic role of CCR2 in DLBCL and demonstrate that targeting CCR2 may be a very promising therapeutic strategy for DLBCL.

In conclusion, we demonstrated that CCR2 is an independent prognostic marker that affects patients with DLBCL and is associated with poorer OS and PFS. Furthermore, we found that CCR2 antagonists inhibited DLBCL cell proliferation and migration and promoted apoptosis in vitro as well as in vivo by activating the PI3K/Akt and p38 MAPK signaling pathways. These discoveries suggest that targeting CCR2 may be a promising treatment option for DLBCL.

#### DATA AVAILABILITY

The datasets used during the current study are available from the corresponding author on reasonable request. All data generated or analyzed during this study are included in this published article.

#### REFERENCES

1. Swerdlow, S. H., Campo, E., Pileri, S. A., Harris, N. L., Stein, H., Siebert, R. et al. The 2016 revision of the World Health Organization classification of lymphoid neoplasms. *Blood* **127**, 2375–2390 (2016).
2. Chihara, T., Wada, N., Ikeda, J., Fujita, S., Hori, Y., Ogawa, H. et al. Frequency of intravascular large B-cell lymphoma in Japan: study of the Osaka Lymphoma Study Group. *J Hematol Oncol* **4**, 14 (2011).
3. Feugier, P., Van Hoof, A., Sebban, C., Solal-Celigny, P., Bouabdallah, R., Fermé, C. et al. Long-term results of the R-CHOP study in the treatment of elderly patients with diffuse large B-cell lymphoma: a study by the Groupe d'Etude des Lymphomes de l'Adulte. *J Clin Oncol* **23**, 4117–4126 (2005).
4. Camicia, R., Winkler, H. C., Hassa, P. O. Novel drug targets for personalized precision medicine in relapsed/refractory diffuse large B-cell lymphoma: a comprehensive review. *Mol Cancer* **14**, 207 (2015).
5. Coiffier, B., Lepage, E., Briere, J., Herbrecht, R., Tilly, H., Bouabdallah, R. et al. CHOP chemotherapy plus rituximab compared with CHOP alone in elderly patients with diffuse large-B-cell lymphoma. *N Engl J Med* **346**, 235–242 (2002).
6. Ghielmini, M., Vitolo, U., Kimby, E., Montoto, S., Walewski, J., Pfreundschuh, M. et al. ESMO Guidelines consensus conference on malignant lymphoma 2011 part 1: diffuse large B-cell lymphoma (DLBCL), follicular lymphoma (FL) and chronic lymphocytic leukemia (CLL). *Ann Oncol* **24**, 561–576 (2013).
7. Perry, A. M., Mitrovic, Z., Chan, W. C. Biological prognostic markers in diffuse large B-cell lymphoma. *Cancer Control* **19**, 214–226 (2012).
8. Salven, P., Orpana, A., Teerenhovi, L., Joensuu, H. Simultaneous elevation in the serum concentrations of the angiogenic growth factors VEGF and bFGF is an independent predictor of poor prognosis in non-Hodgkin lymphoma: a single-institution study of 200 patients. *Blood* **96**, 3712–3718 (2000).
9. Nagarsheth, N., Wicha, M. S., Zou, W. Chemokines in the cancer microenvironment and their relevance in cancer immunotherapy. *Nat Rev Immunol* **17**, 559–572 (2017).
10. Balkwill, F. R. The chemokine system and cancer. *J Pathol* **226**, 148–157 (2012).
11. Brummer, G., Fang, W., Smart, C., Zinda, B., Alissa, N., Berkland, C. et al. CCR2 signaling in breast carcinoma cells promotes tumor growth and invasion by promoting CCL2 and suppressing CD154 effects on the angiogenic and immune microenvironments. *Oncogene* **39**, 2275–2289 (2020).
12. Brummer, G., Acevedo, D. S., Hu, Q., Portsche, M., Fang, W. B., Yao, M. et al. Chemokine Signaling Facilitates Early-Stage Breast Cancer Survival and Invasion through Fibroblast-Dependent Mechanisms. *Mol Cancer Res* **16**, 296–308 (2018).
13. Li, X., Yao, W., Yuan, Y., Chen, P., Li, B., Li, J. et al. Targeting of tumour-infiltrating macrophages via CCL2/CCR2 signalling as a therapeutic strategy against hepatocellular carcinoma. *Gut* **66**, 157–167 (2017).
14. Qian, B. Z., Li, J., Zhang, H., Kitamura, T., Zhang, J., Campion, L. R. et al. CCL2 recruits inflammatory monocytes to facilitate breast-tumour metastasis. *Nature* **475**, 222–225 (2011).
15. Yao, W., Ba, Q., Li, X., Li, H., Zhang, S., Yuan, Y. et al. A Natural CCR2 Antagonist Relieves Tumor-associated Macrophage-mediated Immunosuppression to Produce a Therapeutic Effect for Liver Cancer. *EBioMedicine* **22**, 58–67 (2017).
16. Ding, X., Yang, D. R., Lee, S. O., Chen, Y. L., Xia, L., Lin, S. J. et al. TR4 nuclear receptor promotes prostate cancer metastasis via upregulation of CCL2/CCR2 signaling. *Int J Cancer* **136**, 955–964 (2015).
17. Sanford, D. E., Belt, B. A., Panni, R. Z., Mayer, A., Deshpande, A. D., Carpenter, D. et al. Inflammatory monocyte mobilization decreases patient survival in pancreatic cancer: a role for targeting the CCL2/CCR2 axis. *Clin Cancer Res* **19**, 3404–3415 (2013).
18. Kitamura, T., Qian, B. Z., Soong, D., Cassetta, L., Noy, R., Sugano, G. et al. CCL2-induced chemokine cascade promotes breast cancer metastasis by enhancing retention of metastasis-associated macrophages. *J Exp Med* **212**, 1043–1059 (2015).
19. Husson, H., Carideo, E. G., Cardoso, A. A., Lugli, S. M., Neuberger, D., Munoz, O. et al. MCP-1 modulates chemotaxis by follicular lymphoma cells. *Br J Haematol* **115**, 554–562 (2001).
20. Li, Y. L., Shi, Z. H., Wang, X., Gu, K. S., Zhai, Z. M. Prognostic significance of monocyte chemoattractant protein-1 and CC chemokine receptor 2 in diffuse large B cell lymphoma. *Ann Hematol* **98**, 413–422 (2019).
21. Wagner, E. F., Nebreda, A. R. Signal integration by JNK and p38 MAPK pathways in cancer development. *Nat Rev Cancer* **9**, 537–549 (2009).
22. Alzahrani, A. S. PI3K/Akt/mTOR inhibitors in cancer: At the bench and bedside. *Semin Cancer Biol* **59**, 125–132 (2019).
23. Tewari, D., Patni, P., Bishayee, A., Sah, A. N., Bishayee, A. Natural products targeting the PI3K-Akt-mTOR signaling pathway in cancer: A novel therapeutic strategy. *Semin Cancer Biol* <https://doi.org/10.1016/j.semcancer.2019.12.008> (2019).
24. Li, M. Q., Li, H. P., Meng, Y. H., Wang, X. Q., Zhu, X. Y., Mei, J. et al. Chemokine CCL2 enhances survival and invasiveness of endometrial stromal cells in an autocrine manner by activating Akt and MAPK/Erk1/2 signal pathway. *Fertil Steril* **97**, 919–929 (2012).

25. Korbecki, J., Kojder, K., Simińska, D., Bohatyrewicz, R., Gutowska, I., Chlubek, D. et al. CC Chemokines in a Tumor: A Review of Pro-Cancer and Anti-Cancer Properties of the Ligands of Receptors CCR1, CCR2, CCR3, and CCR4. *Int J Mol Sci* **21** (2020).
26. Wei, J., Fang, D., Zhou, W. CCR2 and PTPRC are regulators of tumor micro-environment and potential prognostic biomarkers of lung adenocarcinoma. *Ann Transl Med* **9**, 1419 (2021).
27. Lu, Y., Cai, Z., Xiao, G., Liu, Y., Keller, E. T., Yao, Z. et al. CCR2 expression correlates with prostate cancer progression. *J Cell Biochem* **101**, 676–685 (2007).
28. Ou, B., Cheng, X., Xu, Z., Chen, C., Shen, X., Zhao, J. et al. A positive feedback loop of  $\beta$ -catenin/CCR2 axis promotesregorafenib resistance in colorectal cancer. *Cell Death Dis* **10**, 643 (2019).
29. Wyler, L., Napoli, C. U., Ingold, B., Sulser, T., Heikenwälder, M., Schraml, P. et al. Brain metastasis in renal cancer patients: metastatic pattern, tumour-associated macrophages and chemokine/chemoreceptor expression. *Br J Cancer* **110**, 686–694 (2014).
30. Vande Broek, I., Leleu, X., Schots, R., Facon, T., Vanderkerken, K., Van Camp, B. et al. Clinical significance of chemokine receptor (CCR1, CCR2 and CXCR4) expression in human myeloma cells: the association with disease activity and survival. *Haematologica* **91**, 200–206 (2006).
31. Sun, C., Li, X., Guo, E., Li, N., Zhou, B., Lu, H. et al. MCP-1/CCR-2 axis in adipocytes and cancer cell respectively facilitates ovarian cancer peritoneal metastasis. *Oncogene* **39**, 1681–1695 (2020).
32. Mitchem, J. B., Brennan, D. J., Knolhoff, B. L., Belt, B. A., Zhu, Y., Sanford, D. E. et al. Targeting tumor-infiltrating macrophages decreases tumor-initiating cells, relieves immunosuppression, and improves chemotherapeutic responses. *Cancer Res* **73**, 1128–1141 (2013).
33. Maxwell, P. J., Neisen, J., Messenger, J. Waugh, D. J. Tumor-derived CXCL8 signaling augments stroma-derived CCL2-promoted proliferation and CXCL12-mediated invasion of PTEN-deficient prostate cancer cells. *Oncotarget* **5**, 4895–4908 (2014).
34. US National Library of Medicine. ClinicalTrials.gov <https://clinicaltrials.gov/ct2/show/NCT01015560> (2015).
35. US National Library of Medicine. ClinicalTrials.gov <https://clinicaltrials.gov/ct2/show/NCT02345408> (2016).
36. Abid, S., Marcos, E., Parpaleix, A., Amsellem, V., Breau, M., Houssaini, A. et al. CCR2/CCR5-mediated macrophage-smooth muscle cell crosstalk in pulmonary hypertension. *Eur Respir J* **54** (2019).
37. Fresno Vara, J. A., Casado, E., de Castro, J., Cejas, P., Belda-Iniesta, C. González-Barón, M. PI3K/Akt signalling pathway and cancer. *Cancer Treat Rev* **30**, 193–204 (2004).
38. Nepstad, I., Hatfield, K. J., Grønningsæter, I. S. Reikvam, H. The PI3K-Akt-mTOR Signaling Pathway in Human Acute Myeloid Leukemia (AML) Cells. *Int J Mol Sci* **21** (2020).
39. Xia, P., Xu, X. Y. PI3K/Akt/mTOR signaling pathway in cancer stem cells: from basic research to clinical application. *Am J Cancer Res* **5**, 1602–1609 (2015).
40. Roca, H., Varsos, Z., Pienta, K. J. CCL2 protects prostate cancer PC3 cells from autophagic death via phosphatidylinositol 3-kinase/AKT-dependent survivin up-regulation. *J Biol Chem* **283**, 25057–25073 (2008).

## ACKNOWLEDGEMENTS

We greatly appreciate Dr. Zhi-Min Zhai and Dr. Shu-Dao Xiong of The Second Affiliated Hospital of Anhui Medical University for providing the experimental platform. We are also thankful to Dr. Ding from The First Affiliated Hospital of USTC for providing the DLBCL cell lines. We also thank Associate Professor Yan-Li Li for her support with statistical analysis. We also recognize the use of a Nanotoxicology platform for the bioluminescent imaging of the tumor-bearing mouse. The authors thank P2 Laboratory Animal Research, College of Basic Medical Sciences, for the excellent animal care (and SPECTRAL Lago and Lago X Imaging System).

## AUTHOR CONTRIBUTIONS

Y.-L.L. designed the research, collected the clinical data, supervised the experiments and revised the manuscript. Q.-Q.H. analyzed the clinical data, performed the experiments in vitro, completed statistical analysis and wrote the paper. Z.-F.W. and Q.-T.H. helped to perform in vivo experiments. Q.L. and Z.-M.Z. also supervised the experiments and revised the manuscript.

## FUNDING

This work was supported by National Natural Science Foundation of China (81700194), College Natural Science Foundation of Anhui Province (KJ2021A0214).

## COMPETING INTERESTS

The authors declare no competing interests.

## ETHICS APPROVAL

This study was approved by the Institutional Review Board of Anhui Medical University and was conducted in accordance with The Code of Ethics of the World Medical Association (Declaration of Helsinki).

## ADDITIONAL INFORMATION

**Correspondence** and requests for materials should be addressed to Yan-Li Li.

**Reprints and permission information** is available at <http://www.nature.com/reprints>

**Publisher's note** Springer Nature remains neutral with regard to jurisdictional claims in published maps and institutional affiliations.